Aquatic Toxicology 206 (2019) 43–53

Contents lists available at ScienceDirect

Aquatic Toxicology

journal homepage: www.elsevier.com/locate/aqtox

Response of natural phytoplankton communities exposed to crude oil and chemical dispersants during a mesocosm experiment

Laura Bretherton[a,*], Manoj Kamalanathan[a], Jennifer Genzer[a], Jessica Hillhouse[a], Samantha Setta[a], Yue Liang[b], Chris M. Brown[b], Chen Xu[c], Julia Sweet[d], Uta Passow[d], Zoe V. Finkel[b], Andrew J. Irwin[e], Peter H. Santschi[c,f], Antonietta Quigg[a,f]

[a] Department of Marine Biology, Texas A&M University at Galveston, Galveston, Texas, United States
[b] Environmental Science Department, Mount Allison University, Sackville, New Brunswick, Canada
[c] Department of Marine Science, Texas A&M University at Galveston, Galveston, Texas, United States
[d] Marine Science Institute, University of California Santa Barbara, Santa Barbara, California, United States
[e] Mathematics and Computer Science Department, Mount Allison University, Sackville, New Brunswick, Canada
[f] Department of Oceanography, Texas A&M University, College Station, Texas, United States

ARTICLE INFO

Keywords:
Aggregates
Community composition
Corexit
Gulf of Mexico
Oil
Photosynthesis
Phytoplankton

ABSTRACT

During the 2010 Deepwater Horizon oil spill, the chemical dispersant Corexit was applied over vast areas of the Gulf of Mexico. Marine phytoplankton play a key role in aggregate formation through the production of extracellular polymeric materials (EPS), an important step in the biological carbon pump. This study examined the impacts of oil and dispersants on the composition and physiology of natural marine phytoplankton communities from the Gulf of Mexico during a 72-hour mesocosm experiment and consequences to carbon export. The communities were treated using the water accommodated fraction (WAF) of oil, which was produced by adding Macondo surrogate oil to natural seawater and mixed for 24 h in the dark. A chemically enhanced WAF (CEWAF) was made in a similar manner, but using a mixture of oil and the dispersant Corexit in a 20:1 ratio as well as a diluted CEWAF (DCEWAF). Phytoplankton communities exposed to WAF showed no significant changes in PSII quantum yield (F_v/F_m) or electron transfer rates (ETR_{max}) compared to Control communities. In contrast, both F_v/F_m and ETR_{max} declined rapidly in communities treated with either CEWAF or DCEWAF. Analysis of other photophysiological parameters showed that photosystem II (PSII) antenna size and PSII connectivity factor were not altered by exposure to DCEWAF, suggesting that processes downstream of PSII were affected. The eukaryote community composition in each experimental tank was characterized at the end of the 72 h exposure time using 18S rRNA sequencing. Diatoms dominated the communities in both the control and WAF treatments (52 and 56% relative abundance respectively), while in CEWAF and DCEWAF treatments were dominated by heterotrophic Euglenozoa (51 and 84% respectively). Diatoms made up the largest relative contribution to the autotrophic eukaryote community in all treatments. EPS concentration was four times higher in CEWAF tanks compared to other treatments. Changes in particle size distributions (a proxy for aggregates) over time indicated that a higher degree of particle aggregation occurred in both the CEWAF and DCEWAF treatments than the WAF or Controls. Our results demonstrate that chemically dispersed oil has more negative impacts on photophysiology, phytoplankton community structure and aggregation dynamics than oil alone, with potential implications for export processes that affect the distribution and turnover of carbon and oil in the water column.

1. Introduction

The Deepwater Horizon (DwH) oil spill resulted in the continuous release of an estimated 4.1 million barrels of crude oil into the northern Gulf of Mexico (GOM) over a span of 84 days during 2010 (Crone and Tolstoy, 2010; McNutt et al., 2012; Reddy et al., 2012). In the months following the spill, mean total polycyclic aromatic hydrocarbon (PAH) concentrations in seawater samples taken from the GOM ranged from 0.2 to 59 mg L^{-1} (Wade et al., 2013; Sammarco et al., 2013). In an attempt to limit coastal damage from slicks, the chemical dispersant Corexit 9500 A and others were applied to surface waters and directly at the wellhead at 1500 m depth (Kujawinski et al., 2011). Corexit

* Corresponding author. Present address: Environmental Science Department, Mount Allison University, Sackville, New Brunswick, Canada.
E-mail address: lbretherton@mta.ca (L. Bretherton).

https://doi.org/10.1016/j.aquatox.2018.11.004
Received 13 July 2018; Received in revised form 31 October 2018; Accepted 5 November 2018
Available online 06 November 2018
0166-445X/

contains surfactant molecules that reduce surface tension at the water-oil interface, and can therefore reduce the size of oil slicks by allowing them to mix with the water's surface (Lessard and DeMarco, 2000). A total of 6.8 million liters of Corexit was applied to the GOM; this event also marked the first time dispersants had been discharged in deep waters (Lehr et al., 2010; Kujawinski et al., 2011).

The effects of crude oil exposure on marine phytoplankton remain unclear, and a variety of reported responses exists in the literature. Certainly, many studies have reported that oil has an inhibitory effect on algal growth (Hsiao et al., 1970; Østgaard et al., 1984; Hook and Osborn, 2012; Garr et al., 2014; Bretherton et al., 2018) and motility (Garr et al., 2014), can disrupt cell membranes (Hook and Osborn, 2012) and interfere with synthesis and maintenance of nucleic acids (Deasi et al., 2010). However, others have demonstrated that some phytoplankton are unaffected (Harrison et al., 1986; Bretherton et al., 2018) or even stimulated (González et al., 2009; Özhan et al., 2014a; Bretherton et al., 2018) by the presence of crude oil. The most toxic components of oil, the PAHs, may stimulate ($\sim 1\ mg\ L^{-1}$) or inhibit ($\sim 100\ mg\ L^{-1}$) phytoplankton growth depending on concentration (Harrison et al., 1986). Phytoplankton community composition in the GOM changed following the DwH spill (Parsons et al., 2015). Mesocosm studies with natural phytoplankton communities support these observations, often finding either diatoms (González et al., 2009; Gilde and Pinckney, 2012; Özhan and Bargu, 2014) or phytoflagellates (Adekunle et al., 2010; Özhan et al., 2014b) becoming the dominant taxa following exposure to oil.

Phytoplankton produce extracellular polymeric substances (EPS), including transparent exopolymer particles (TEP), which promote the formation of aggregates (Passow et al., 1994; Kiørboe, 2001; Quigg et al., 2016). The production of EPS is affected by photosynthetic rate and overall health of phytoplankton cells and further varies across taxa and with cell size (Claquin et al., 2008). Oil is incorporated into aggregates, forming sinking marine oil snow (MOS), a phenomenon that was observed following the DwH incident (Passow et al., 2012; Daly et al. 2016). While the sedimentation of oil-laden MOS is helpful in removing oil from surface waters, it can have detrimental effects on benthic organisms (White et al., 2012; Baguley et al., 2015). The effect of oil and Corexit-dispersed oil on phytoplankton health thus potentially affects the fate of oil, because the physiological state of phytoplankton changes their EPS and TEP production (Liu and Buskey, 2000; Wolfstein and Stal, 2002; Kahl et al., 2008) and thus the potential to form MOS. Direct effects of WAF and CEWAF on phytoplankton and the secondary effects of aggregation and sinking can be expected to lead to changes in the taxonomic and size structure of the community. This in turn will have feedback effects on TEP and MOS production. Few studies measure the influence of oil and dispersant on phytoplankton photophysiology outside of the quantum yield of photochemistry (González et al., 2009, 2013; Bretherton et al., 2018). Other parameters generated with these tools can give a better picture about the nature of oil toxicity, and therefore the overall health of the phytoplankton.

We exposed natural communities of phytoplankton found in the northern GOM to both a water accommodated fraction (WAF) of oil and mixtures of oil and dispersants (chemically enhanced WAF; CEWAF) over a 72 h period to monitor short-term changes in photosynthesis using fluorescence signals from photosystem II (PSII). Single-turnover PSII fluorescence was used to derive the PSII quantum yield (F_v/F_m), PSII antenna size (σ_{PSII}) and PSII connectivity factor (ρ). Pulse-amplitude modulation (PAM) fluorescence was used to derive relative maximum electron transfer rates ($rETR_{max}$) to assess a suite of photophysiological parameters. We combined this data with molecular techniques to assess the eukaryote community, and measurements of EPS and TEP as well as particle dynamics to examine changes in phytoplankton communities as they respond to oil and dispersants. Distinct responses were observed between treatments, as well as shifts in community structure. We assess underlying mechanisms that may explain these changes using mesocosms, and relate these findings to MOS formation.

2. Methods and materials

2.1. Mesocosm set-up

Water was collected ~80 km off the coast of Louisiana in the GOM (29° 22′52″ N, 93° 23′06″ W) on July 16 2016, with in situ temperature (30.5 °C), salinity (31.13 ppt) and pH (8.02) recorded using a calibrated water quality sonde probe (Hydrolab MS 5, Hach, Loveland, CO). The seawater was taken back to land for experimentation at Texas A&M University at Galveston. Twelve 100 L mesocosm tanks were filled with each of the four treatments (final volume 87 L) prepared in triplicate: control (seawater only), a water accommodated fraction (WAF) of oil, a chemically enhanced water accommodated fraction (CEWAF), and a 10-fold diluted CEWAF (DCEWAF), as described in Wade et al. (Wade et al., 2017). Briefly, the WAF was prepared by mixing 25 mL (5 mL every 30 min for 2.5 h) of Macondo surrogate oil (MC252) into 130 L of seawater in a baffled recirculating tank. Gentle mixing ended 24 h after the initial oil addition, and the WAF was transferred to the treatment tanks. To produce CEWAF, Corexit was mixed with MC252 oil in a ratio of 1:20 and then 25 mL of this mixture (5 ml every 30 min for 2.5 h) was added to 130 L of seawater and again mixed for ~24 h before transfer to the treatment tanks. DCEWAF was prepared by diluting CEWAF 10-fold with the original seawater. This work was performed in dim light at ambient room temperatures (~21 °C) immediately prior to starting the experiment. All tanks had nutrients (nitrate, phosphate, silicate and trace metals) added at f/20 concentrations (Guillard et al. 1975), and maintained at an irradiance of $\sim 50\ \mu mol\ m^{-2}\ s^{-1}$. The mesocosm tanks themselves were not mixed for the duration of the experiment so as not to disrupt the formation of aggregates, or impact the formation of EPS and TEP.

Estimated oil equivalents (EOE) were used to determine the starting WAF, CEWAF and DCEWAF concentrations in mesocosm tanks, following the method previously described in Wade et al. (2013). Briefly, 5 mL control or treated seawater was diluted with dichloromethane to extract the oil, and approximately 4 mL of the dichloromethane fraction of each sample was transferred into a cuvette for EOE analysis. EOE was measured spectrofluorometrically, and the optimum excitation and emission wavelengths for EOE determinations were 260 and 358 nm respectively, as in Wade et al. (2013). Initial EOE concentrations ranged from 0.29 to 81.01 $mg\ L^{-1}$, which is within the range measured off the Louisiana coast following the DwH spill (Sammarco et al., 2013).

2.2. Chlorophyll fluorescence measurements

Samples (4 mL) were taken from each mesocosm tank every 12 h (between 0900–1000 hours and 2100–2200 hours) and dark-acclimated for 15 min. This period of dark-acclimation assumes all PSII reaction centers become open, yielding a minimum fluorescence (F_o) value. The samples were then placed in a Fluorescence Induction and Relaxation (FIRe) fluorometer (Satlantic, Halifax, Canada), which exposes algal samples to a saturating pulse of blue light for 80 μs, closing all PSII reaction centers and yielding a maximum fluorescence (F_m) value. The difference between the F_m and F_o values is the variable fluorescence (F_v), and changes in F_v relative to F_m (F_v/F_m) are a measure of photosynthetic efficiency, also termed the maximum quantum yield of PSII. The fluorometer plots fluorescence yield over time (μs), generating a single turnover (ST) curve. From this, other parameters such as PSII antenna size (σ_{PSII}) and PSII connectivity factor (ρ) can be derived (Kolber et al., 1998). The FIRe fluorometer was set to 80 μs ST flashes with a 60 μs relaxation phase. Each sample was run for 40 iterations to reduce noise and produce a smoother curve. A blank sample was run for each treatment (0.7 μm GF/F filtered seawater from each treatment) to subtract any background fluorescing entities (e.g. CDOM, Corexit) from the F_o and F_m values respectively (Cullen and David, 2003).

Additionally, these parameters were recorded for samples before WAF and CEWAF production began (−24 h time point).

A pulse-amplitude modulation (PAM) fluorometer (Phyto-PAM EDF, Walz) was used to measure relative maximum electron transfer rates ($rETR_{max}$). Every 24 h, a sample (4 mL) was placed in the Phyto-PAM after dark-acclimation for 15 min to obtain relative maximum electron transfer rates ($rETR_{max}$) by performing rapid light curves (RLC). A total of 8 light steps were used (16, 32, 64, 164, 264, 364, 464, 564, 664, 764 µmol photons m^{-2} s^{-1}). These measurements were performed each morning (between 0900–1200 hours). The PHYTO-PAM utilizes light pulses composed of four different colors; blue (470 nm), green (520 nm), light red (645 nm) and dark red (665 nm). Excitation of chlorophyll fluorescence by multiple wavelengths allows phytoplankton taxa with different light-harvesting pigments to be distinguished. Phycocyanin and allophycocyanin, pigments found in the cyanobacteria, are both strongly excited by red (645 nm) light, but not by blue (470 nm). Brown algae are excited strongly by blue (470 nm) and green (520 nm) light due to the presence of pigments such as fucoxanthin and carotenoids, though further distinction of the signal between groups (such as diatoms versus dinoflagellates) is not possible using this technique. Finally, green algae are effectively excited by all wavelengths except for green light (520 nm). For further detail, see Schreiber (1998). Samples from FIRe analysis were then placed in a 10 AU Turner fluorometer to obtain in situ chlorophyll concentrations. Blanks were also run to remove interference from background fluorescence. The relative fluorescence values were recorded for each sample and converted to chlorophyll-*a* concentrations using a standard curve. The fluorometer was calibrated using a standard of chlorophyll-*a* extracted from the alga *Anacystis nodulans* (Sigma-Aldrich) diluted with 90% acetone to concentrations between 0.2–80 µg L^{-1} following the EPA method 445.0 (Arar and Collins, 1997).

2.3. Microbial eukaryote community composition

The estimate of the relative abundance of active microbial eukaryotes within and across treatments is based on 18S RNA sequences from RNAseq data and reflects the relative presence, activity, and detectability of each species. RNA was extracted from each of the 12 mesocosm tanks at the end of the experiment after 72 h. Aliquots (250 to 4000 mL) were rapidly (no longer than 20 min.) and gently filtered onto two 47 mm, 0.8 µm polycarbonate filters. The filters and denaturating solution (Ambion Totally RNA kit, Thermo Fisher AM1910) were added to Y-matrix bead beater tubes (MoBio) and the samples lysed using a SuperFastprep2 bead beater (30 s at the maximum setting) and immediately stored in a -80 °C freezer. RNA was extracted by exposing samples immediately after thawing to two additional 30 s rounds in the SuperFastprep2 bead beater, with 60 s on ice in between rounds. The Ambion Totally RNA kit was used to extract RNA followed by DNA removal with the Ambion Turbo DNAfree kit (ThermoFisher AM1907) as per manufacturer instructions.

RNA was sequenced as 125 base pair paired-end reads using Illumina HiSeq 250 RNAseq by the McGill University and Génome Québec Innovation Centre, Montréal, Canada. PolyA selection was used to remove the majority of the rRNA using the NEBNext Poly(A) mRNA magnetic isolation module kit from New England Biolabs. Approximately 2–10% of the original rRNA sequences pass through this step and are sequenced (Abernathy and Overturf, 2016). Trimmomatic was used to remove Illumina adapters and low quality bases were identified using Phred scores (Bolger et al., 2014). Kraken and the Silva SSU rRNA Ref NR 99 database (release 123) were used to filter reads matching 18S sequences (Quast et al., 2013; Wood and Salzberg, 2014). Kallisto and Sleuth were used to match, count and perform relative abundance analysis for reads against the Silva 18S database (Bray et al., 2016; Pimentel et al., 2017). RNA yields in some of the CEWAF and DCEWAF samples were low.

Each 18S sequence in the Silva database was identified with an accession code and a hierarchical taxonomic identification. All Metazoa, Embryophyta, and non-Eukaryota sequences were removed from the analyses. The taxonomic identification in Silva is hierarchical but the identifications do not all have the same number of levels in the hierarchy so the phylum, order, or class, for example, are not readily extracted. Where possible we used the taxonomic hierarchy found in the World Registry of Marine Species (WoRMS, marinespecies.org) in 2016/17. The genus and species name for each taxon in the Silva database (the last entry in the hierarchy) was used to search WoRMS. A variety of secondary sources were used to identify the taxonomic hierarchy for taxa without a match in WoRMS including the Global Names Index (GNI), the Pan-European Species Infrastructure (PESI), the Paleobiology database (Paleo), and Wikipedia/Wikispecies. The automatic search for all taxa was performed using lifewatch.be on December 31 2016 using WoRMS, GNI, PESI, and Paleo.

2.4. Microscopic identification

A 100 mL sample was taken from each tank after 72 h and settled for 24 h in an Utermohl chamber (Combined Plate Chamber, Hydro-Bios, Germany) fitted with a 100 mL cylinder. The plate was then placed under an inverted light microscope (Motic AE31, BC, Canada) for phytoplankton identification using the ×40 magnification. Phytoplankton observed on the plate were identified to genus level whenever possible using the identification key by Tomas (Tomas, 1997). The presence of aggregates and their associated phytoplankton, if present, were noted. The first 100 cells (or up to 20 fields of view if there were fewer than 100 cells) were identified in each sample.

2.5. EPS and TEP measurements

EDTA-extractable EPS was measured in each tank at the end of the mesocosm (72 h after the start of the experiment). EPS in the suspended particulate matter (SPM) and colloidal fraction (3 kDa- 0.4 µm) were measured and expressed as the sum of neutral sugar, uronic acid, and protein concentrations of these two fractions (Xu et al., 2011). More specifically, SPM was collected by filtering 1–2 L of seawater from each tank through a 0.4 µm polycarbonate membrane, and the particles retained on the membrane were extracted with 1% EDTA at 4 °C for 3 h on an orbital shaker at 150 rpm. The excess EDTA and salts were then removed by ultrafiltering the extractant through an Amicon Ultra-15 centrifugal filter unit with an ultracel-3 membrane (Millipore, 3 kDa). EPS in the colloidal fraction was directly purified (without EDTA extraction) by ultrafiltering the < 0.4 µm fraction through an Amicon Ultra-15 centrifugal filter unit. Neutral sugar content was determined with the anthrone method, with glucose as the standard (Yemm and Willis, 1954). Protein concentrations were measured with Pierce BCA protein assay, with bovine serum albumin (BSA) as the standard (Smith et al., 1985). Analysis of uronic acids was carried out by adding sodium borate (75 mM) in concentrated sulfuric acid and *m*-hydroxydiphenyl, with glucuronic acid as the standard for this assay (Blumenkrantz and Asboe-Hansen, 1973). Total EPS production in the water column was reported as the sum of protein, carbohydrates and uronic acid concentrations in suspended and colloidal particles.

Samples for measuring TEP were collected every 12 h and measured according to Passow and Alldredge (1995). For each tank triplicate samples were gently filtered onto a 0.4 µm polycarbonate filter and stained with a pre-filtered, calibrated Alcian Blue (AB) solution (0.5 g AB and 1.5 mL acetic acid in 50 mL deionized water). Filtered volume varied depending upon the amount of suspended particles (80–120 mL), and was adjusted to maximize the amount of material captured while minimizing filter clogging. Filters were rinsed with deionized water before being stored at −20 °C. To quantify TEP, each filter was acidified with 80% H_2SO_4 for 4 h and the absorbance of the resulting solution was measured on a spectrophotometer at 787 nm. Measurements were calibrated against a Gum Xanthan standard, meaning TEP

concentration is expressed as μg Xanthan equivalent (Xeq.) per liter.

The presence of Corexit interferes with the Alcian Blue staining, resulting at times in artificially elevated values of "TEP". No consistent correction factor could be developed, because it appears that binding of Corexit to TEP depends on the presence of DOM, its quality and quantity. Thus, no TEP values are presented for DCEWAF, but a qualitative evaluation based on our measurements and tests is given. Measurements in CEWAF treatments, were not attempted because previous work showed that the high Corexit concentrations in these treatments led to significant measurement artifacts.

2.6. Particle counts

A 20 mL sample was taken from each mesocosm tank every 24 h, and immediately analyzed using a Coulter counter (Beckman-Coulter, Z2) fitted with a 100 μm aperture. Particle concentrations were measured in three size fractions; 5–10 μm, 10–20 μm and 20–50 μm. The particle coincidence at the aperture was monitored to ensure it remained below 5%. Particle coincidence is an instance of more than one particle entering the aperture simultaneously, which can underestimate particle counts. Samples where particle concentrations were high enough to cause particle coincidence of > 5% were diluted with filtered seawater (0.2 μm, nylon), and only ever happened in CEWAF tanks.

2.7. Statistical analysis

A one-way repeated measures ANOVA was conducted to compare the effects of oil treatment on chlorophyll, F_v/F_m, σ_{PSII}, ρ, and $rETR_{max}$ using the 'psycho' package in 'R' (v 3.5.1). Post-hoc comparisons using a contrast analysis were conducted, and *p*-values were adjusted using the Bonferroni procedure to account for multiple comparisons. A summary of the *p*-values for each between-treatment comparison for each physiological parameter is presented in Table 3.

3. Results

3.1. Oil concentrations

Estimated oil equivalents (EOE) were used to determine the starting oil concentration in the WAF, CEWAF and DCEWAF mesocosm tanks. They were 0.29 (± 0.02) mg L^{-1}, 8.13 (± 0.56) mg L^{-1}, and 81.06 (± 11.83) mg L^{-1}, respectively with 0.41 (± 0.0) mg L^{-1} measured in the controls (Table 1). These concentrations declined exponentially over the 72 h mesocosms following first-order kinetics (see Wade et al., 2017 for details) so that the concentrations at the end of the experiment were 0.026 (± 0.00) mg L^{-1}, 1.84 (± 0.65) mg L^{-1}, and 19.83 (± 0.75) mg L^{-1}, in the WAF, CEWAF and DCEWAF mesocosm treatments respectively (Table 1).

Table 1
Summary of the EOE (estimated oil equivalency, mg L^{-1}), F_v/F_m (dimensionless), chlorophyll *a* (Chl-a, μg L^{-1}) total EPS production (extracellular polymeric substances, mg L^{-1}) and EPS protein:CHO in each treatment after 72 h. Values are means with standard error in brackets, except for EPS data where replicates were pooled and values have a 15% margin of error. N/A indicates values were below detection limits.

Treatment	EOE (Start)	EOE (End)	F_v/F_m	Chl-a	Total EPS	Protein:CHO
Control	0.041 (0.00)	0.007 (0.00)	0.691 (0.09)	1.81 (0.89)	0.540	1.27
WAF	0.29 (0.02)	0.026 (0.00)	0.665 (0.02)	1.96 (0.87)	0.550	1.27
DCEWAF	8.13 (0.56)	1.84 (0.65)	0.321 (0.02)	0.57 (0.06)	0.572	1.48
CEWAF	81.06 (11.83)	19.83 (0.75)	0.047 (0.02)	N/A (—)	2.23	2.35

3.2. Phytoplankton biomass and photophysiology

The trends in chlorophyll *a* concentration over time showed three distinct responses in the treatments (Fig. 1). Chlorophyll concentrations in the control and WAF treatments increased over time, reaching their peak at 60 h, with final concentrations at 72 h of 1.81 and 1.96 μg L^{-1} respectively. In the DCEWAF treatment, chlorophyll concentrations initially increased at 12 h, but from 24 h onwards, remained stable (< 1 μg L^{-1}) and had a final concentration of 0.57 μg L^{-1} after 72 h. There were no significant differences in chlorophyll concentrations observed between Control, WAF and DCEWAF tanks (Table 3). Chlorophyll was not detectable in the CEWAF treatment after 24 h; the fluorescence intensity was at the detection limit and around the same value as that of the blank (CEWAF media made with filtered seawater).

Trends in PSII quantum yield (F_v/F_m) followed a similar pattern to chlorophyll (Fig. 2). In both control and WAF treatments, F_v/F_m increased over time to > 0.6 at 72 h, and there was no significant difference between these two treatments (Table 3). In the DCEWAF treatment, F_v/F_m started increasing at 24 h, but by 48 h it began decreasing to a final value of ~0.35. From 48 h onward, the CEWAF treatment no longer produced reliable variable fluorescence signals, consistent with chlorophyll concentrations falling below the detection limits.

PSII antenna size (σ_{PSII}) was highly constrained within treatments for the duration of the mesocosm experiment (Fig. 2), and ranged between 150-200 $Å^2$ $(quanta)^{-1}$ across all treatments except for CEWAF, where PSII antenna size was 2-fold higher. The PSII connectivity factor (ρ) fluctuated between 0.3 and 0.55 over the 72 h time course in all the treatments, except for CEWAF (Fig. 2). In the CEWAF tanks, the connectivity factor remained below 0.25, except for the final time point. Here, it increased to 0.4, but given the high degree of standard error associated with this time point, it is not likely this represents a real recovery in PSII connectivity. Both σ_{PSII} and ρ showed no significant difference between Control, WAF and DCEWAF (Table 3).

Relative electron transfer rates ($rETR_{max}$) mirrored the trends in chlorophyll and F_v/F_m (Fig. 3). $rETR_{max}$ increased over time in both Control and WAF treatments to ~125 μmol electrons m^{-2} s^{-1} by 72 h, and there was no significant difference between these two treatments (Table 3). $rETR_{max}$ in the DCEWAF treatment remained stable, but an order of magnitude less than Control and WAF values, ranging between 10–25 μmol electrons m^{-2} s^{-1} over the 72 h experiment. The $rETR_{max}$ values in CEWAF tanks were near detection limits (< 1) of the instrument.

3.3. Eukaryote microbial community structure

The Control and WAF tanks had similar microbial eukaryotic community composition and differed substantially from the CEWAF and DCEWAF tanks (Fig. 4). The Control and WAF tanks were dominated by the Bacillariophyta (diatoms) (52 and 56% relative abundance, respectively) while the CEWAF and DCEWAF tanks were dominated by Euglenozoa (51 and 84% relative abundance, respectively). *Skeletonema* spp. represented 17 and 23% of the relative abundance in the Control and WAF tanks, respectively. Other diatom genera that made up more than 0.5% of the relative abundance in both the Control and WAF tanks include: *Thalassiosira*, *Porosira*, and *Cyclotella*. Heterotrophic biflagellated bodonids, including *Neobodo*, dominated the Euglenozoa in the CEWAF and DCEWAF tanks. Other groups high in relative abundance in both the Control and WAF tanks included the Basidiomycota fungi (12 and 14% of the relative abundance, respectively), Oomycota or water molds (9 and 10%), Chlorophyta or green algae (2.9 and 3.0%), and the Dinophyceae or dinoflagellates (1.9 and 1.8%). The Control tanks were higher in relative abundance in Amoebozoa (13 vs. 0.3%) than the WAF tanks. Relative to the CEWAF tanks, the DCEWAF tanks were higher in relative abundance by an order or magnitude or more in Bigyra and Chrysophyceae and lower in relative abundance by

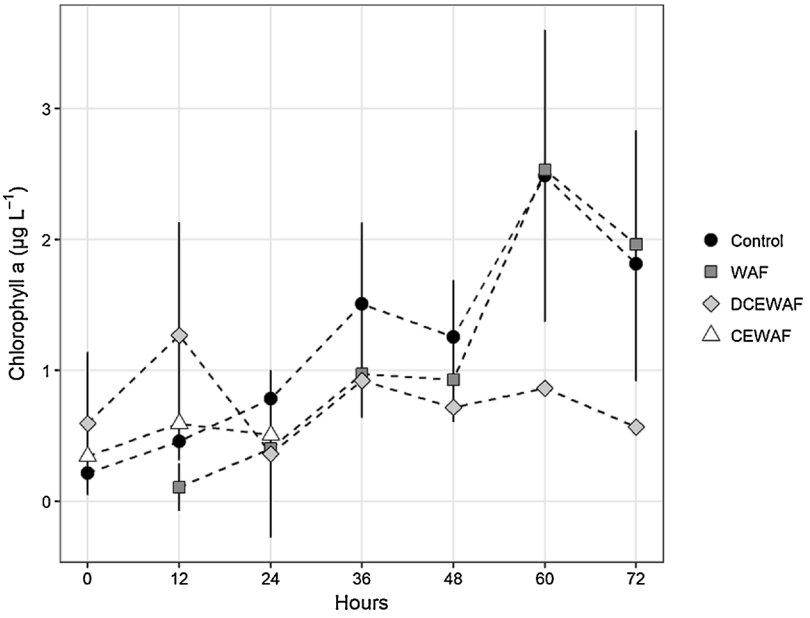

Fig. 1. Chlorophyll *a* (µg L^{-1}) in control, WAF, DCEWAF and CEWAF tanks over 72 h. Missing values indicate time points where measurements fell below detection limit (only occurred in CEWAF tanks). Error bars are +/- standard error (n = 3).

more than an order or magnitude in the Amoebozoa. Many of dominant Chrysophyceae genera identified, for example *Paraphysomonas*, were heterotrophic. *Amphidinium* was the dominant dinoflagellate genus identified in the mesocosms and *Nannochloris* and *Picochlorum* were the dominant green algae genera identified in the CEWAF tanks.

The major photosynthetic eukaryotes in the mesocosms (with > 0.5% relative abundance in any treatment) belonged to the diatoms, green algae, and dinoflagellate groups. Only the diatoms are strictly autotrophic, the green algae and dinoflagellates include mixotrophic and heterotrophic species. In total, these taxonomic groups constituted 56 and 61% of the relative abundance of the 18S signal in the Control and WAF tanks, respectively, and 16 and 7% of the relative abundance in the CEWAF and DCEWAF tanks, respectively. Diatoms were 92%, dinoflagellates 3% and green algae 5% of the relative abundance of the primarily photosynthetic groups in both the Control and WAF tanks, 74%, 7% and 20% in the CEWAF tanks, and 39%, 10% and 51% in the DCEWAF tanks.

A total of 12 diatom genera were identified microscopically across all mesocosm tanks, and are summarized in Table 2. The most genera were observed in the Control tanks, with 11 of the 12 occurring in these tanks, and 4 unique to the Controls (*Coscinodiscus*, *Thalassiosira*, *Stephanopyxis* and *Thalassionema*). The large pennate diatom genus *Lioloma* was uniquely observed in DCEWAF tanks. A total of 4 genera were observed in all treatments; *Chaetoceros*, *Pseudo-nitzschia*, *Skeletonema* and *Navicula*. The dominance of diatoms in the mesocosm communities was a consistent outcome of both the molecular and microscopic analyses. The microscopic approach identified several genera abundant to the GOM.

3.4. EPS, TEP and particle size distribution

Total (particle associated plus colloidal) EDTA-extractable EPS concentration was highest in CEWAF tanks (2.23 mg L^{-1}), and similar in all other treatments (~0.55 mg L^{-1}) at the end of the mesocosm experiment (Table 1). The protein:CHO ratio in the EDTA-extractable EPS of the CEWAF treatments was higher than in other treatments.

Total TEP concentration was consistently higher in WAF compared to Control treatments (Fig. 5), increasing slightly over time in the WAF treatment and decreasing over time in the Control treatment, until during the last twelve hours when TEP concentrations in the WAF treatment dropped to levels similar to those in the controls. Measured "TEP" values in DCEWAF were more than twice as high as in the Control, and 1.5 times higher than in WAF. We do not know exactly which fraction of these higher "TEP" values were due to artifacts caused by the interference of Corexit with the method, but methodological test suggest that the interference in DCEWAF treatments were small.

Marine snow and marine oil snow accounted for the largest (> 0.5 mm) and most visible particles in all treatments. Herein, we examined the smaller particulate material (< 100 µm) associated with EPS, TEP and other aggregation behavior (see Quigg et al., 2016 for descriptions and definitions). Temporal development of particle concentrations varied by treatment, as did the relative contribution of specific size classes (Fig. 6). Over time the CEWAF and DCEWAF tanks were characterized by a decrease in the smallest size fraction (5–10 µm) and an increase in the larger fraction (10–20 µm and 20–50 µm), with an overall decrease in total particle concentrations. Total particles concentrations in the control and WAF increased over time, as do particle concentrations in the smallest size fraction, while the larger size fraction decreased.

4. Discussion

4.1. Impact of oil and Corexit-dispersed oil on photophysiology

As a result of the DwH incident, phytoplankton were exposed to oil and oil-dispersant mixtures in the GOM. While there are many studies examining the response of bacterial communities, few studies have focused on phytoplankton (Parsons et al., 2015). In many algal oil studies, an examination of the response of the photophysiological apparatus is absent. In our study, the phytoplankton community was particularly robust to oil exposure in WAF treatments, showing no significant differences in photophysiology relative to the Control treatment. Both of these treatments exhibited an increase in F_v/F_m with time. Changes in F_v/F_m can be caused by increased light availability, changes in nutrients, and shifts in taxonomic and size structure (Gorbunov et al., 2001; Moore et al., 2008; Suggett et al., 2009). Light limitation occurs in the northern GOM due to heavy particulate loading from the Mississippi and Atchafalaya Rivers, which reduces light penetration in the water column (Quigg et al., 2011). Alleviation of light limitation in both Control and WAF tanks would not be surprising given

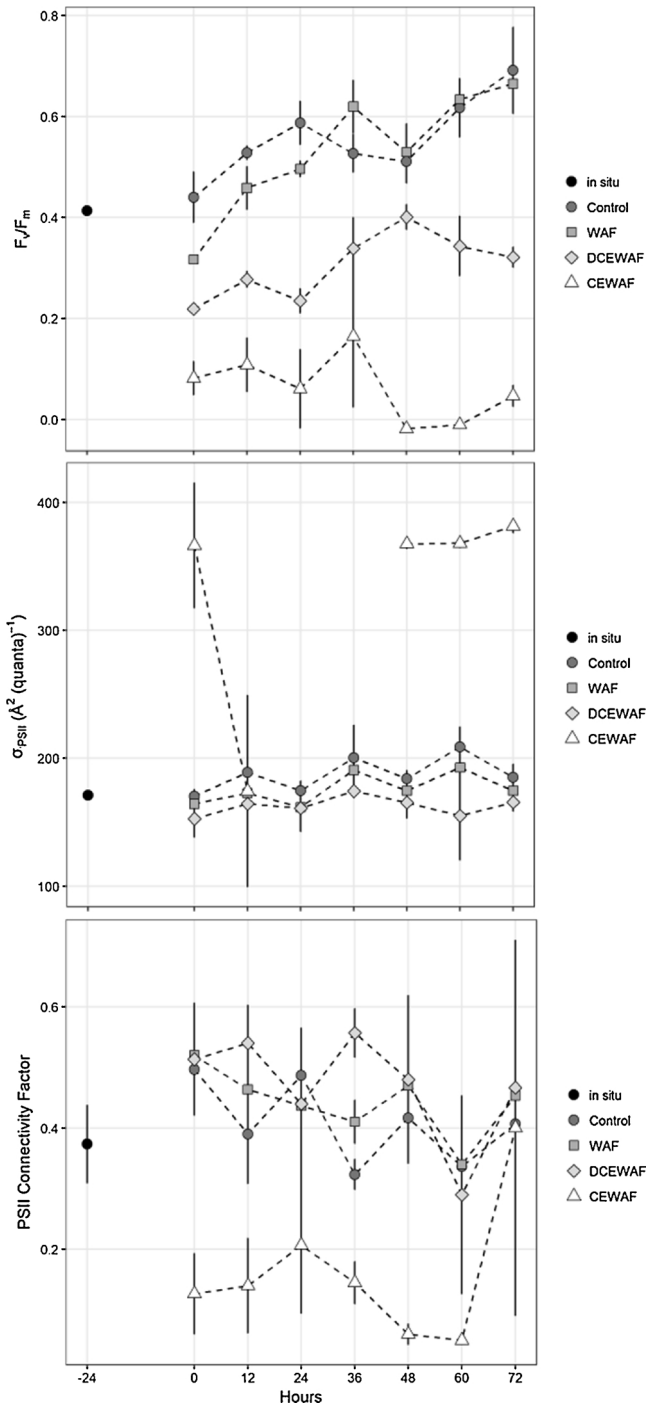

Fig. 2. Quantum yield (F_v/F_m), PSII antenna size (σ_{PSII}, Å^2 (quanta)$^{-1}$) and PSII connectivity factors (ρ, dimensionless) measured in control, WAF, DCEWAF and CEWAF tanks over 72 h. Missing values indicate time points where the fluorometer was unable to fit value (only occurred in CEWAF). Error bars represent +/- standard error (n = 3). Data points at -24 h indicate measurements made on the seawater before WAF/CEWAF production began.

the turbid nature of coastal waters off the coast of Louisiana where the seawater for this experiment was collected (Rowe and Chapman, 2002). Further, the addition of nutrients at the start of the mesocosm experiment could also explain the overall increase in F_v/F_m observed in the Control, WAF, and to a smaller extent the DCEWAF tanks. Despite significant nitrogen loading by the Mississippi River in the spring, phytoplankton in the northern GOM can be frequently found to be nitrogen and/or phosphate limited (Quigg et al., 2011), therefore it is possible that nutrient addition had some effect on the temporal trend of F_v/F_m.

In contrast to the WAF and control treatments, the chemically dispersed oil (CEWAF, DCEWAF treatments) had clear detrimental effects on the health of the microalgae, visible in terms of both biomass and photosynthesis responses. In the CEWAF treatment, F_v/F_m reached the detection limit for the FIRe fluorometer after 48 h, indicating that this treatment was lethal (EOE = 81.06 mg L^{-1}). The DCEWAF treatment (EOE = 8.13 mg L^{-1}) depressed both F_v/F_m and $rETR_{max}$ to levels below those of the Control and WAF treatments by 72 h, suggesting that photosynthesis was slowed or became more inefficient. However, both PSII antenna size and connectivity factor did not significantly differ from control and WAF tanks, which would suggest that PSII in the DCEWAF-treated phytoplankton either retained functionality or was repaired at a very fast rate. Additionally, the seawater in both the CEWAF and DCEWAF treatments was more opaque due to the higher oil concentration, and could have limited light penetration in these tanks, and thus altered F_v/F_m.

Based on these results, we hypothesize that exposure to chemically dispersed oil causes some interruption to photosynthesis. Dispersant application enhances the solubility of polycyclic aromatic hydrocarbons (PAHs) and increases their concentration in the water column (Yamada et al., 2003). PAHs are known to be toxic to many aquatic organisms such as fish (Ramachandran et al., 2006; Carls et al., 2008) and zooplankton (Almeda et al., 2013). Some PAHs such as anthracene may degrade into quinones that can influence electron transfer chains (Hammel, 1995). Exposure to anthracene causes decreased ETR_{max} and inhibition of electron flow in the alga *Chlamydomonas reinhardtii* (Aksmann and Tukaj, 2008), and benzoquinones (similar to the photodegradation products of some PAHs) can oxidize the plastoquinone pool (Srivastava et al., 1995). While the degradation of PAHs such as anthracene was not monitored, the bacterial community in the DCEWAF tanks were enriched with OTUs belonging to a group of known PAH-degraders (Doyle et al., 2018).

It is unlikely that anthracene, or any products of its degradation, interact directly with PSII. Instead, these compounds likely cause membrane damage that results in proton leakage from the thylakoid (Aksmann et al., 2011). Work on the model diatom *Thalassiosira pseudonana* has shown that a variety of PAHs can cause membrane damage (Bopp and Lettieri, 2007; Carvalho et al., 2011). Additionally, when the pennate diatom *Phaeodactylum tricornutum* was exposed to WAF and CEWAF in a previous study, it showed signs of membrane damage in the CEWAF only (Hook and Osborn, 2012). When exposed to WAF, CEWAF, and DCEWAF, a decline in F_v/F_m is only observed in the dispersed oil treatments in a variety of phytoplankton (Bretherton et al., 2018), consistent with the present study. Thus, membrane damage through PAH exposure could explain why F_v/F_m and $rETR_{max}$ declined in the DCEWAF tanks and not in those treated with WAF.

Given that we worked at concentrations of WAF and (D)CEWAF which were likely present after the spill (Wade et al., 2013; Sammarco et al., 2013), these findings can also help us to understand the short term impacts of oil and dispersant exposure on phytoplankton physiology. Given their pelagic nature and high turnover times, direct detrimental effects to GOM phytoplankton in the long-term would not be expected. However, as phytoplankton physiology indirectly affects aggregation and sedimentation events through mass die-offs, these short-term perturbations could still have long-term consequences for the export and fate of oil. Nonetheless, more work needs to be performed to develop a clearer understanding of these phenomena.

4.2. Impact of oil and Corexit-dispersed oil on community composition

Changes in fluorescence signals from natural phytoplankton communities can also be indicative of changes in community composition (Suggett et al., 2009). Typically, F_v/F_m values are high and σ_{PSII} values are low in well-mixed coastal environments that are dominated by

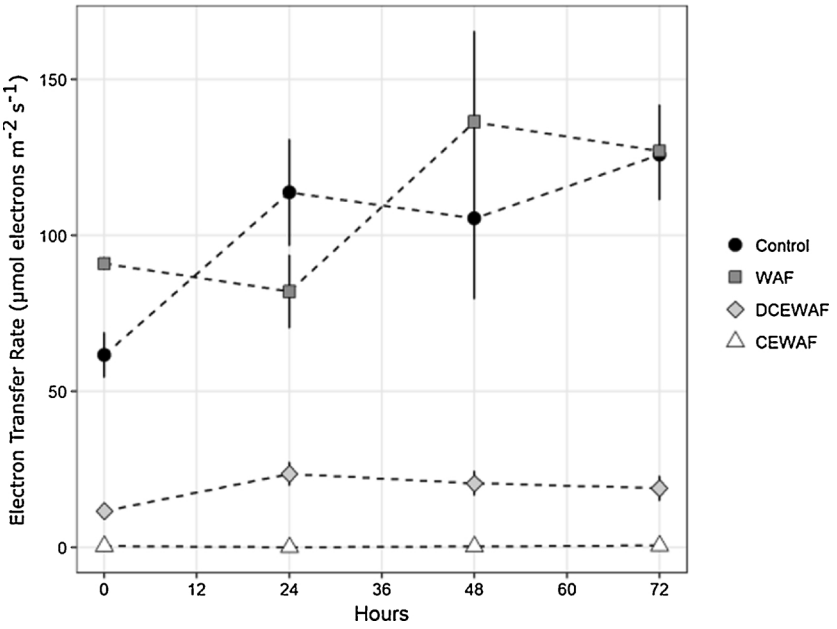

Fig. 3. Relative maximum electron transfer rates ($rETR_{max}$, µmol photons m^{-2} s^{-1}) obtained from rapid light curves in control, WAF, DCEWAF and CEWAF tanks over 72 h. Rapid light curves were taken every 24 h. Error bars represent +/- standard error (n = 3).

diatoms (Moore et al., 2005), consistent with the heavily diatom dominated communities found in the Control and WAF tanks (Fig. 4, Table 2). A decline in F_v/F_m and increase in σ_{PSII} can be characteristic of waters dominated by smaller flagellates (Aiken et al., 2004), as observed in the CEWAF and DCEWAF tanks (Fig. 4). However, the Euglenozoa in these treatments were mostly represented by the heterotrophic bodonids (Von Der Heyden et al., 2004), and would not contribute to the fluorescence signal. In both the Control and the WAF tanks, phytoplankton (diatoms, dinoflagellates and green algae) made up over half the eukaryote community, and were dominated by diatoms, while in the CEWAF and DCEWAF communities diatoms contributed only 16% and 7%, respectively. In the latter two treatments, diatom relative abundance decreased, while both the dinoflagellates and green algae increased. These results are typical of mesocosm studies, where WAF exposure often results in no change or an increase in the relative abundance of diatoms (González et al., 2009; Jung et al., 2012; Özhan and Bargu, 2014), whereas chemically dispersed oil treatments frequently lead to a decline in the diatom population, and an increase in dinoflagellates, green algae and other flagellated eukaryotes (Gilde and Pinckney, 2012).

Four diatom genera were identified from microscopy samples in all treatments; *Chaetoceros*, *Skeletonema*, *Navicula* and *Pseudo-nitzschia*

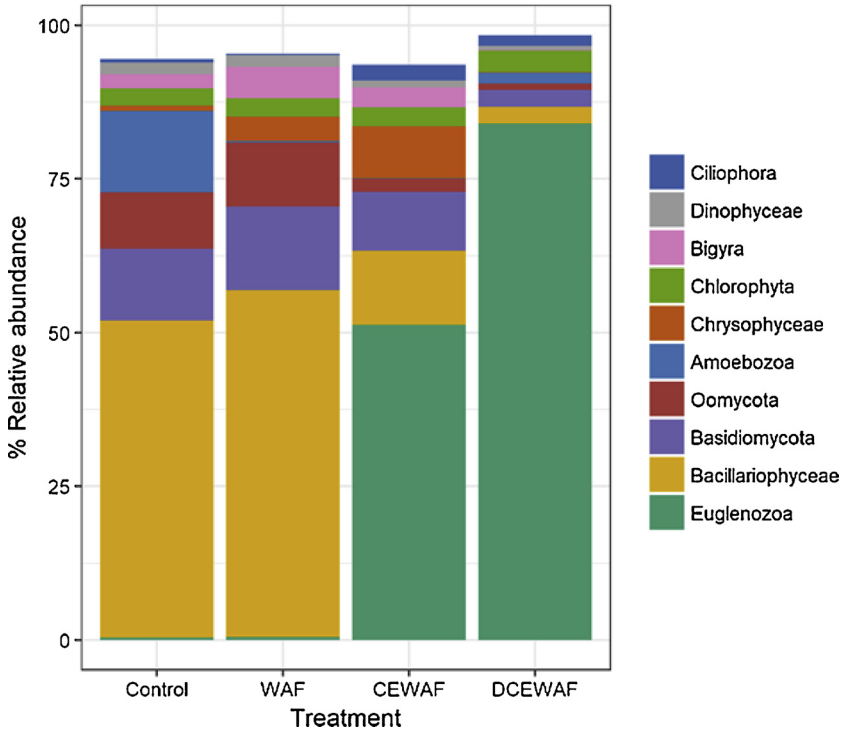

Fig. 4. Percent relative abundance of the of the top 10 microbial eukaryotic groups across treatments after 72 h of exposure.

Table 2
Diatom genera identified in each treatment across all replicates under an inverted light microscope. Samples were taken after 72 h of exposure in mesocosm tanks.

	Control	WAF	DCEWAF	CEWAF
Centric	*Chaetoceros* *Skeletonema* *Coscinodiscus* *Thalassiosira*	*Chaetoceros* *Skeletonema*	*Chaetoceros* *Skeletonema*	*Chaetoceros* *Skeletonema*
Pennate	*Navicula* *Pseudo-nitzschia* *Cylindrotheca* *Nitzschia* *Synedra* *Stephanopyxis* *Thalassionema*	*Navicula* *Pseudo-nitzschia* *Cylindrotheca* *Nitzschia* *Synedra*	*Navicula* *Pseudo-nitzschia* *Cylindrotheca* *Nitzschia* *Synedra* *Lioloma*	*Navicula* *Pseudo-nitzschia*

(Table 2). These genera typically contribute significantly to GOM phytoplankton communities (Strom and Strom, 1996; Macintyre et al., 2011). The oil responses of these genera have also been studied in mesocosm experiments, which have shown varied, species-specific results (see Ozhan et al., 2014a for a summary). For example, a previous study found that Corexit-dispersed oil caused a dramatic increase in the relative abundance of *Chaetoceros septentrionalis* (15.5% in Control to 65–70% in treated tanks), but had a negative effect on *S. costatum* (25% in Control to < 1% in treated tanks) (Siron et al., 1996). In another mesocosm experiment, *Chaetoceros diadema* only became dominant in tanks treated with just oil, and was out-competed by other diatoms in the dispersed oil treatments, while *Skeletonema*. cf. *marinoi*'s relative abundance declined in all treatments, even the Control (Jung et al., 2012). Interestingly, there was a bloom of *Skeletonema* (of unknown species) in the GOM after the spill was over (August/ September 2010), identified through sediment traps (Yan et al., 2016). These diverse responses suggest that the response to oil and dispersed oil are species-specific, and therefore the changes in diatom genera observed in our mesocosm experiment are likely dictated by the representative species that were present in the starting community for each genus.

The diatom genus *Pseudo-nitzschia* was observed in all treatments in this mesocosm study (see Table 2). Little has been published on the oil tolerance of *Pseudo-nitzschia*. In a mesocosm experiment using phytoplankton from the GOM, it consistently became the dominant pennate diatom genus in WAF with EOE concentrations ranging from 2.5 to 5.2 mg L^{-1}, and its abundance increased further with nutrient enrichment (Ozhan and Bargu 2014). Following the DwH spill, *Pseudo-nitzschia spp*. abundance did not fluctuate from its pre-spill baseline (Parsons et al., 2015).

Pseudo-nitzschia blooms in the GOM typically occur in spring conditions when Si:N ratios are low (Parsons et al., 2013) as it is a lightly silicifying diatom (Sommer, 1994). *Pseudo-nitzschia* may produce the neurotoxin domoic acid (Bates et al. 1989), and toxic blooms of *Pseudo-nitzschia* do occur in the GOM (Dortch et al. 1997, Liefer et al. 2009, Parsons et al., 2013). Off the coast of Alabama, *Pseudo-nitzschia* blooms were found to be a result of increased dissolved inorganic carbon and salinity, and decreased silica concentrations that favored a change in phytoplankton community composition: *Pseudo-nitzschia* dominated, and co-occurred with *Chaetoceros* and *Skeletonema* (Macintyre et al., 2011). Conditions that promote the growth of *Pseudo-nitzschia* could increase the likelihood of toxic blooms occurring in the GOM.

Top-down control from grazing could also be a contributing factor to changes in phytoplankton community composition since zooplankton were not excluded from the experiment due to logistical constraints. Oil and dispersant exposure can be very detrimental to zooplankton mortality and diversity (Almeda et al., 2013, 2014b), and can impair the swimming ability of some taxa such as copepods (Cohen et al., 2014). While grazing rates were not measured, observations from microscopy and the 18S data suggest that grazers did not make up a significant portion of the eukaryote community.

4.3. Diatom aggregate formation

Diatoms are known to form large (> 0.5 mm) aggregates (Beers et al., 1986; Alldredge and Gotschalk, 1989) and produce TEP (Passow et al., 1994; Claquin et al., 2008). Marine snow sized diatom aggregates, which scavenge dispersed and dissolved oil from the water, lead to the formation of MOS, as observed following the DwH spill (Passow et al., 2012, 2017; Yan et al., 2016). It is estimated that 4–31% of DwH oil was exported to the sediment via sinking MOS (Chanton et al., 2015; Daly et al., 2016). In our study, TEP production was higher in the WAF treatment relative to the Control treatment, indicating that TEP production may be a common response of diatoms to WAF exposure. While we were unable to accurately measure TEP in the DCEWAF treatments, our data does suggest that TEP concentrations were elevated compared to WAF. Other evidence suggests that aggregation was indeed elevated in both CEWAF and DCEWAF treatments.

In the DCEWAF and CEWAF tanks total particle concentrations declined over time, but the concentration of particles in the largest size fraction (10–50 µm) increased, suggesting that smaller particles may have aggregated. The Coulter counter data can only sample small aggregates (≤ 50 µm), and our sampling scheme would have precluded the identification of marine snow sized aggregates. However, as aggregation theory elucidates, large aggregates form through successive collisions of smaller aggregates, and the appearance of such micro-aggregates is a required first step towards the formation of marine snow sized, sinking aggregates (Jackson and Burd, 1998). The TOC content of material collected from the bottom of these tanks at the end of the experiment was consistently higher in the CEWAF treatments compared to controls and WAF treatments (see Kamalanathan et al., 2018), suggesting much more aggregation occurred. Low PSII electron transport capacity and efficiency, formation of micro-aggregates and the appearance of marine snow sized aggregates in the DCEWAF and CEWAF treatments all suggest that the presence of Corexit-dispersed oil led to decreased phytoplankton health associated with increased aggregation.

In contrast, increased particle concentrations in the Control and

Table 3
Output of repeated-measures ANOVA with contrast analysis for chlorophyll, F_v/F_m, σ_{PSII}, ρ and $rETR_{max}$ over time. *P*-values have been adjusted using the Bonferroni method; * indicates where *p* is 0.01 – 0.05, ** where *p* is 0.001 – 0.01, and *** where *p* is less than 0.001.

	P-value				
Comparison	Chlorophyll	F_v/F_m	σ_{PSII}	ρ	$rETR_{max}$
Control –WAF	1.000	1.000	1.000	1.000	1.000
Control – CEWAF	0.042 (*)	0.000 (***)	0.002 (**)	0.000 (***)	0.000 (***)
Control – DCEWAF	1.000	0.002 (**)	1.000	0.490	0.002 (**)
WAF –CEWAF	0.091	0.000 (***)	0.001 (***)	0.000 (***)	0.000 (***)
WAF – DCEWAF	1.000	0.003 (**)	1.000	1.000	0.003 (**)
CEWAF – DCEWAF	0.226	0.008 (**)	0.001 (***)	0.000 (***)	1.000

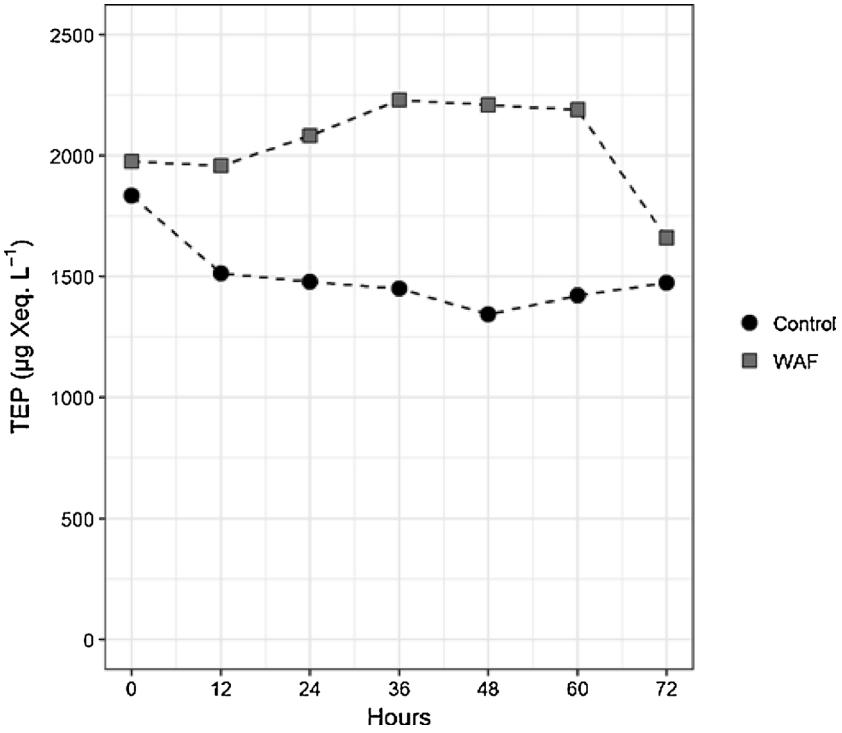

Fig. 5. Transparent exopolymeric particles (TEP, µg Xeq. L^{-1}) measured in control and WAF tanks over 72 h. Data was not collected for DCEWAF and CEWAF.

WAF treatments was largely driven by increases in the smallest size fraction (Fig. 6), and was likely due to higher rates of cell division given the trends in chlorophyll *a* concentration, F_v/F_m and $rETR_{max}$ over time. We thus suggest that particle dynamics in Control and WAF treatments were dominated by growth in the smallest size fraction, while in DCEWAF and possibly CEWAF changes in particle size distributions were dominated by aggregation. Enhanced aggregation in the presence of Corexit-dispersed oil appears to directly contradict results from rolling tank experiments that showed an inhibitive effect on MOS formation in treatments containing Corexit and oil, because the Corexit dispersed the TEP (Passow et al., 2017). In contrast to the mesocosm experiments presented here, oil and Corexit were added directly to rolling tanks, rather than first making CEWAF which was added to phytoplankton. Interactions between Corexit and EPS that control TEP formation depend on exposure and concentration. Aggregation of diatoms is highly species specific (Crocker and Passow, 1995), and aggregate sinking velocity depends – among other things - on aggregate composition, density and packaging (Ploug et al., 2008; Iversen and Ploug, 2010). Hence, community shifts caused by oil and/or dispersant exposure impact not only the rate of aggregate formation, but also aggregate sinking velocities, and thus how effectively those aggregates may export oil through the water column.

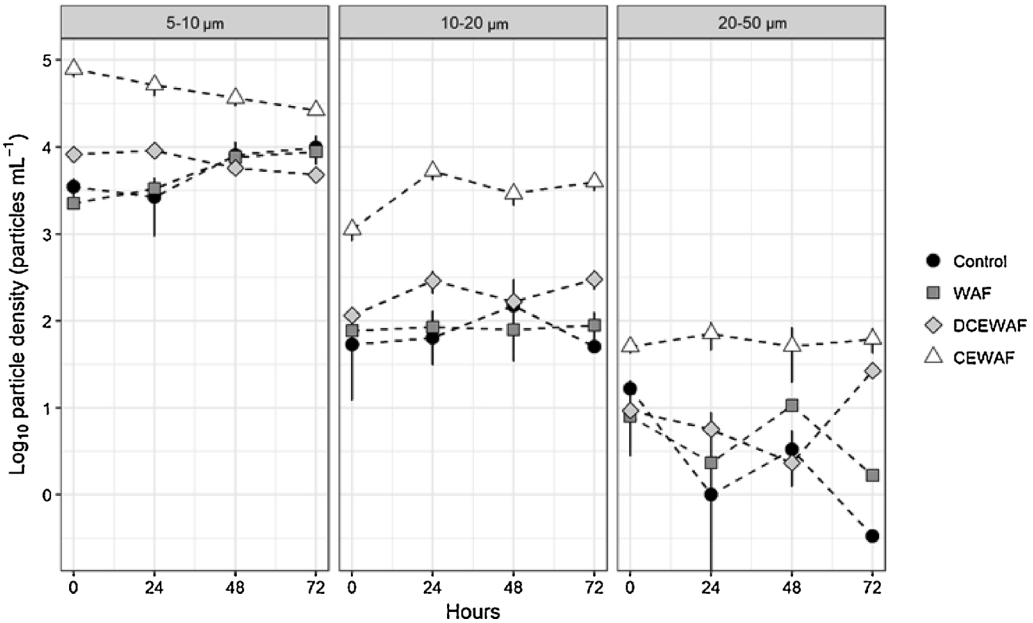

Fig. 6. Log_{10} particle density in three size fractions (5–10 µm, 10–20 µm, and 20–50 µm) over time in Control, WAF, DCEWAF and CEWAF tanks, collected using a Coulter counter. Error bars are +/- standard error (n = 3).

4.4. Conclusions and outlook

Studies on the base of the food web such as this are important to understanding the consequences of oil spills and dispersant application to higher trophic levels. We see the largest negative effects on the phytoplankton communities in the treatments that included Corexit in addition to oil (CEWAF and DCEWAF), with fewer effects observed in oil-only treatments (WAF). This is in agreement with previous toxicological studies on phytoplankton and crude oil (Hook and Osborn, 2012; Jung et al., 2012; Özhan and Bargu, 2014; Bretherton et al., 2018). Photophysiological evidence suggests that the CEWAF and DCEWAF treatments may negatively affect the electron transport chain. This is more likely to be a result of oxidation of the plastoquinone pool rather than direct disruption of photosystem II. The treatment effects appear to be species-specific, leading to changes in phytoplankton community and size structure, which may have influenced TEP production and rates of aggregation. While it is known that there were phytoplankton blooms following the DwH spill (Yan et al., 2016; Hu et al. 2011), it remains unknown if long-term changes occurred in phytoplankton communities of the GOM. Changes in phytoplankton may have been transient and the negative effects offset by a decrease in predation (Abbriano et al., 2011). However, transient changes in phytoplankton may have cascaded up the food web through bioaccumulation (Almeda et al., 2013, 2014a) and may change oil distribution by causing sedimentation events.

Acknowledgements

This research was supported by a grant from The Gulf of Mexico Research Initiative to support consortium research entitled ADDOMEx (Aggregation and Degradation of Dispersants and Oil by Microbial Exopolymers) Consortium. The original data can be found at the Gulf of Mexico Research Initiative Information and Data Cooperative (GRIIDC) at http://data.gulfresearchinitiative.org (doi: https://doi.org/10.7266/N7NP22G2; https://doi.org/10.7266/N7028PMG; https://doi.org/10.7266/N7RV0M1R; https://doi.org/10.7266/N7CF9NK6; https://doi.org/10.7266/N7JD4V8Z). Metadata for the metatranscriptomes are available at the NCBI BioSample database (http://www.ncbi.nlm.nih.gov/biosample/) under accession number SAMN08118040.

References

Abbriano, R.M., Carranza, M.M., Hogle, S.L., Levin, R.A., Netburn, A.N., Seto, K.L., Snyder, S.M., Franks, P.J.S., 2011. Deepwater horizon oil spill: a review of the planktonic response. Oceanography 24, 294–301. https://doi.org/10.2307/24861323.

Abernathy, J., Overturf, K., 2016. Comparison of ribosomal RNA removal methods for transcriptome sequencing workflows in teleost fish. Anim. Biotechnol. 27, 60–65. https://doi.org/10.1080/10495398.2015.1086365.

Adekunle, I.M., Ajijo, M.R., Adeofun, C.O., Omoniyi, I.T., 2010. Response of four phytoplankton species found in some sectors of Nigerian coastal waters to crude oil in controlled ecosystem. Int. J. Environ. Res. 4, 65–74. https://doi.org/10.22059/IJER.2010.157.

Aiken, J., Fishwick, J., Moore, G., Pemberton, K., 2004. The annual cycle of phytoplankton photosynthetic quantum efficiency, pigment composition and optical properties in the western English Channel. J. Mar. Biol. Assoc. U.K. 84, 301–313. https://doi.org/10.1017/S0025315404009191h.

Aksmann, A., Shutova, T., Samuelsson, G., Tukaj, Z., 2011. The mechanism of anthracene interaction with photosynthetic apparatus: A study using intact cells, thylakoid membranes and PS II complexes isolated from Chlamydomonas reinhardtii. Aquat. Toxicol. 104, 205–210. https://doi.org/10.1016/j.aquatox.2011.04.017.

Aksmann, A., Tukaj, Z., 2008. Intact anthracene inhibits photosynthesis in algal cells: a fluorescence induction study on *Chlamydomonas reinhardtii* cw92 strain. Chemosphere 74, 26–32. https://doi.org/10.1016/j.chemosphere.2008.09.064.

Alldredge, A.L., Gotschalk, C.C., 1989. Direct observations of the mass flocculation of diatom blooms: characteristics, settling velocities and formation of diatom aggregates. Deep Sea Res. Part A Oceanogr. Res. Pap. 36, 159–171. https://doi.org/10.1016/0198-0149(89)90131-3.

Almeda, R., Connelly, T.L., Buskey, E.J., 2014a. Novel insight into the role of heterotrophic dinoflagellates in the fate of crude oil in the sea. Sci. Rep. 4, 7560. https://doi.org/10.1038/srep07560.

Almeda, R., Hyatt, C., Buskey, E.J., 2014b. Toxicity of dispersant Corexit 9500A and crude oil to marine microzooplankton. Ecotoxicol. Environ. Saf. 106, 76–85. https://doi.org/10.1016/j.ecoenv.2014.04.028.

Almeda, R., Wambaugh, Z., Chai, C., Wang, Z., Liu, Z., Buskey, E.J., 2013. Effects of crude oil exposure on bioaccumulation of polycyclic aromatic hydrocarbons and survival of adult and larval stages of gelatinous zooplankton. PLoS One 8, e74476. https://doi.org/10.1371/journal.pone.0074476.

Arar, E.J., Collins, G.B., 1997. In Vitro Determination of Chlorophyll a and Pheophytin a in Marine and Freshwater Algae by Fluorescence. Environmental Protection Agency, Washington 22 pp.

Baguley, J., Montagna, P., Cooksey, C., et al., 2015. Community response of deep-sea soft-sediment metazoan meiofauna to the Deepwater Horizon blowout and oil spill. Mar. Ecol. Prog. Ser. 528, 127–140. https://doi.org/10.3354/meps11290.

Beers, J.R., Trent, J.D., Reid, F.M.H., Shanks, A.L., 1986. Macroaggregates and their phytoplanktonic components in the Southern California Bight. J. Plankton Res. 8, 475–487. https://doi.org/10.1093/plankt/8.3.475.

Blumenkrantz, N., Asboe-Hansen, G., 1973. New method for quantitative determination of uronic acids. Anal. Biochem. 54, 484–489. https://doi.org/10.1016/0003-2697(73)90377-1.

Bolger, A.M., Lohse, M., Usadel, B., 2014. Trimmomatic: A flexible trimmer for Illumina sequence data. Bioinformatics 30, 2114–2120. https://doi.org/10.1093/bioinformatics/btu170.

Bopp, S.K., Lettieri, T., 2007. Gene regulation in the marine diatom Thalassiosira pseudonana upon exposure to polycyclic aromatic hydrocarbons (PAHs). Gene 396, 293–302. https://doi.org/10.1016/j.gene.2007.03.013.

Bray, N.L., Pimentel, H., Melsted, P., Pachter, L., 2016. Near-optimal probabilistic RNA-seq quantification. Nat. Biotechnol. 34, 525–527. https://doi.org/10.1038/nbt.3519.

Bretherton, L., Williams, A., Genzer, J., Hillhouse, J., Kamalanathan, M., Finkel, Z.V., Quigg, A., 2018. Physiological response of 10 phytoplankton species exposed to macondo oil and the dispersant. Corexit. J. Phycol. 54 (3), 317–328. https://doi.org/10.1111/jpy.12625.

Carls, M.G., Holland, L., Larsen, M., Collier, T.K., Scholz, N.L., Incardona, J.P., 2008. Fish embryos are damaged by dissolved PAHs, not oil particles. Aquat. Toxicol. 88, 121–127. https://doi.org/10.1016/j.aquatox.2008.03.014.

Carvalho, R.N., Bopp, S.K., Lettieri, T., 2011. Transcriptomics responses in marine diatom thalassiosira pseudonana exposed to the polycyclic aromatic hydrocarbon Benzo[a]pyrene. PLoS One 6, e26985. https://doi.org/10.1371/journal.pone.0026985.

Chanton, J., Zhao, T., Rosenheim, B.E., et al., 2015. Using natural abundance radiocarbon to trace the flux of petrocarbon to the seafloor following the deepwater horizon oil spill. Environ. Sci. Technol. 49, 847–854. https://doi.org/10.1021/es5046524.

Claquin, P., Probert, I., Lefebvre, S., Veron, B., 2008. Effects of temperature on photosynthetic parameters and TEP production in eight species of marine microalgae. Aquat. Microb. Ecol. 51, 1–11. https://doi.org/10.3354/ame01187.

Cohen, J.H., McCormick, L.R., Burkhardt, S.M., 2014. Effects of dispersant and oil on survival and swimming activity in a marine copepod. Bull. Environ. Contam. Toxicol. 92, 381–387. https://doi.org/10.1007/s00128-013-1191-4.

Crocker, K.M., Passow, U., 1995. Differential aggregation of diatoms. Mar. Ecol. Prog. Ser. 117, 249–258. https://doi.org/10.3354/meps117249.

Crone, T.J., Tolstoy, M., 2010. Magnitude of the 2010 Gulf of Mexico oil leak. Science 330, 634. https://doi.org/10.1126/science.1195840.

Cullen, J.T., David, R.F., 2003. The blank can make a big difference in oceanographic measurements. Limnol. Oceanogr. Bull. 12, 29–34. https://doi.org/10.1002/lob.200413229.

Daly, K.L., Passow, U., Chanton, J., Hollander, D., 2016. Assessing the impacts of oil-associated marine snow formation and sedimentation during and after the Deepwater Horizon oil spill. Anthropocene 13, 18–33. https://doi.org/10.1016/j.ancene.2016.01.006.

Deasi, S.R., Verlecar, X.N., Ansari, Z.A., Jagtap, T.G., Sarkar, A., Vashistha, D., Dalal, S.G., 2010. Evaluation of genotoxic responses of *Chaetoceros tenuissimus* and *Skeletonema costatum* to water accommodated fraction of petroleum hydrocarbons as biomarker of exposure. Water Res. 44, 2235–2244. https://doi.org/10.1016/j.watres.2009.12.048.

Doyle, S.M., Whitaker, E.A., De Pascuale, V., Wade, T.L., Knap, A.H., Santschi, P.H., Quigg, A., Sylvan, J.B., 2018. Rapid formation of microbe-oil aggregates and changes in community composition in coastal surface water following exposure to oil and the dispersant corexit. Front. Microbiol. 9. https://doi.org/10.3389/fmicb.2018.00689.

Garr, A.L., Laramore, S., Krebs, W., 2014. Toxic effects of oil and dispersant on marine microalgae. Bull. Environ. Contam. Toxicol. 93, 654–659. https://doi.org/10.1007/s00128-014-1395-2.

Gilde, K., Pinckney, J.L., 2012. Sublethal effects of crude oil on the community structure of estuarine phytoplankton. Estuar. Coasts 35, 853–861. https://doi.org/10.1007/s12237-011-9473-8.

González, J., Fernández, E., Figueiras, F.G., Varela, M., 2013. Subtle effects of the water soluble fraction of oil spills on natural phytoplankton assemblages enclosed in mesocosms. Estuar. Coast. Shelf Sci. 124, 13–23. https://doi.org/10.1016/j.ecss.2013.03.015.

González, J., Figueiras, F.G., Aranguren-Gassis, M., Crespo, B.G., Fernández, E., Morán, X.A.G., Nieto-Cid, M., 2009. Effect of a simulated oil spill on natural assemblages of marine phytoplankton enclosed in microcosms. Estuar. Coast. Shelf Sci. 83, 265–276. https://doi.org/10.1016/j.ecss.2009.04.001.

Gorbunov, M.Y., Kolber, Z.S., Lesser, M.P., Falkowski, P.G., 2001. Photosynthesis and photoprotection in symbiotic corals. Assoc. Sci. Limnol. Oceanogr. 46, 75–85. https://doi.org/10.4319/lo.2001.46.1.0075.

Hammel, K.E., 1995. Mechanisms for polycyclic aromatic hydrocarbon degradation by ligninolytic fungi. Environ. Health Perspect. 41–43 National Institute of Environmental Health Science.

Harrison, P.J., Cochlan, W.P., Acreman, J.C., Parsons, T.R., Thompson, P.A., Dovey, H.M., Xiaolin, C., 1986. The effects of crude oil and Corexit 9527 on marine phytoplankton in an experimental enclosure. Mar. Environ. Res. 18, 93–109. https://doi.org/10.

1016/0141-1136(86)90002-4.
Hook, S.E., Osborn, H.L., 2012. Comparison of toxicity and transcriptomic profiles in a diatom exposed to oil, dispersants, dispersed oil. Aquat. Toxicol. 124–125, 139–151. https://doi.org/10.1016/j.aquatox.2012.08.005.
Hsiao, S.I.C., Kittle, D.W., Foy, M.G., 1978. Effects of crude oils and the oil dispersant corexit on primary production of arctic marine phytoplankton and seaweed. Environ. Pollut. 15, 209–221. https://doi.org/10.1016/0013-9327(78)90066-6. 1970.
Hu, C., Weisberg, R.H., Liu, Y., Zheng, L., Daly, K.L., English, D.C., Zhao, J., Vargo, G.A., 2011. Did the northeastern Gulf of Mexico become greener after the Deepwater Horizon oil spill? Geophys. Res. Lett. 38, L09601. https://doi.org/10.1029/2011GL047184.
Iversen, M.H., Ploug, H., 2010. Ballast minerals and the sinking carbon flux in the ocean: carbon-specific respiration rates and sinking velocity of marine snow aggregates. Biogeosciences 7, 2613–2624. https://doi.org/10.5194/bg-7-2613-2010.
Jackson, G.A., Burd, A.B., 1998. Aggregation in the marine environment. Environ. Sci. Technol. 32, 2805–2814. https://doi.org/10.1021/es980251w.
Jung, S.W., Kwon, O.Y., Joo, C.K., Kang, J.H., Kim, M., Shim, W.J., Kim, Y.O., 2012. Stronger impact of dispersant plus crude oil on natural plankton assemblages in short-term marine mesocosms. J. Hazard. Mater. 217–218, 338–349. https://doi.org/10.1016/j.jhazmat.2012.03.034.
Kahl, L., Vardi, A., Schofield, O., 2008. Effects of phytoplankton physiology on export flux. Mar. Ecol. Prog. Ser. 354, 3–19. https://doi.org/10.3354/meps07333.
Kiørboe, T., 2001. Formation and fate of marine snow : small-scale processes with large-scale implications. Sci. Mar. 65, 57–71. https://doi.org/10.3989/scimar.2001.65s257.
Kolber, Z.S., Prasil, O., Falkowski, P.G., 1998. Measurements of variable chlorophyll fluorescence using fast repetition rate techniques: defining methodology and experimental protocols. Biochim. Biophys. Acta – Bioenerg. 1367, 88–106. https://doi.org/10.1016/S0005-2728(98)00135-2.
Kujawinski, E.B., Kido Soule, M.C., Valentine, D.L., Boysen, A.K., Longnecker, K., Redmond, M.C., 2011. Fate of dispersants associated with the Deepwater Horizon oil spill. Environ. Sci. Technol. 45, 1298–1306. https://doi.org/10.1021/es103838p.
Lehr, B., Bristol, S., Possolo, A., 2010. Oil budget calculator—Deepwater horizon. Report to the National Incident Command: Federal Interagency Solutions Group.
Lessard, R., DeMarco, G., 2000. The significance of oil spill dispersants. Spill Sci. Technol. Bull. 6, 59–68. https://doi.org/10.1016/S1353-2561(99)00061-4.
Liu, H., Buskey, E.J., 2000. Hypersalinity enhances the production of extracellular polymeric substance (EPS) in the Texas brown tide alga, Aureoumbra lagunensis (Pelagophyceae). J. Phycol. 36, 71–77. https://doi.org/10.1046/j.1529-8817.2000.99076.x.
Macintyre, H.L., Stutes, A.L., Smith, W.L., Dorsey, C.P., Abraham, A., Dickey, R.W., 2011. *Pseudo- spp.* in the northern Gulf of Mexico. J. Plankton Res. 33, 273–295.
McNutt, M.K., Camilli, R., Crone, T.J., Guthrie, G.D., Hsieh, P.A., Ryerson, T.B., Savas, O., Shaffer, F., 2012. Review of flow rate estimates of the Deepwater Horizon oil spill. Proc. Natl. Acad. Sci. 109, 20260–20267. https://doi.org/10.1073/pnas.1112139108.
Moore, C.M., Lucas, M.I., Sanders, R., Davidson, R., 2005. Basin-scale variability of phytoplankton bio-optical characteristics in relation to bloom state and community structure in the Northeast Atlantic. Deep Sea Res. Part I Oceanogr. Res. Pap. 52, 401–419. https://doi.org/10.1016/j.dsr.2004.09.003.
Moore, C.M., Mills, M.M., Langlois, R., Milne, A., Achterberg, E.P., La Roche, J., Geider, R.J., 2008. Relative influence of nitrogen and phosphorous availability on phytoplankton physiology and productivity in the oligotrophic sub-tropical North Atlantic Ocean. Limnol. Oceanogr. 53, 291–305. https://doi.org/10.4319/lo.2008.53.1.0291.
Østgaard, K., Eide, I., Jensen, A., 1984. Exposure of phytoplankton to ekofisk crude oil. Mar. Environ. Res. 11, 183–200. https://doi.org/10.1016/0141-1136(84)90045-X.
Özhan, K., Bargu, S., 2014. Distinct responses of Gulf of Mexico phytoplankton communities to crude oil and the dispersant Corexit® EC9500A under different nutrient regimes. Ecotoxicology 23, 370–384. https://doi.org/10.1007/s10646-014-1195-9.
Özhan, K., Miles, S.M., Gao, H., Bargu, S., 2014a. Relative Phytoplankton growth responses to physically and chemically dispersed South Louisiana sweet crude oil. Environ. Monit. Assess. 186, 3941–3956. https://doi.org/10.1007/s10661-014-3670-4.
Özhan, K., Parsons, M.L., Bargu, S., 2014b. How were phytoplankton affected by the deepwater horizon oil spill? BioScience 64, 829–836. https://doi.org/10.1093/biosci/biu117.
Parsons, M.L., Dortch, Q., Doucette, G.J., 2013. An assessment of *Pseudo-nitzschia* population dynamics and domoic acid production in coastal Louisiana. Harmful Algae 30, 65–77. https://doi.org/10.1016/j.hal.2013.09.001.
Parsons, M.L., Morrison, W., Rabalais, N.N., Turner, R.E., Tyre, K.N., 2015. On the Louisiana shelf Phytoplankton and the Macondo oil spill: a comparison of the 2010 phytoplankton assemblage to baseline conditions. Environ. Pollut. 207, 152–160. https://doi.org/10.1016/j.envpol.2015.09.019.
Passow, U., Alldredge, A.L., 1995. A dye-binding assay for the spectrophotometric measurement of transparent exopolymer particles (TEP). Limonol. Oceanogr. 40, 1326–1335. https://doi.org/10.4319/lo.1995.40.7.1326.
Passow, U., Alldredge, A.L., Logan, B.E., 1994. The role of particulate carbohydrate exudates in the flocculation of diatom blooms. Deep. Sea Res. Part I Oceanogr. Res. Pap. 41, 335–357. https://doi.org/10.1016/0967-0637(94)90007-8.
Passow, U., Sweet, J., Quigg, A., 2017. How the dispersant Corexit impacts the formation of sinking marine oil snow. Mar. Pollut. Bull August 12.
Passow, U., Ziervogel, K., Asper, V., Diercks, A., 2012. Marine snow formation in the aftermath of the Deepwater Horizon oil spill in the Gulf of Mexico. Environ. Res. Lett. 7, 035301. https://doi.org/10.1088/1748-9326/7/3/035301.
Pimentel, H., Bray, N.L., Puente, S., Melsted, P., Pachter, L., 2017. Differential analysis of RNA-seq incorporating quantification uncertainty. Nat. Methods 14, 687–690. https://doi.org/10.1038/nmeth.4324.
Ploug, H., Iversen, M.H., Fischer, G., 2008. Ballast, sinking velocity, and apparent diffusivity within marine snow and zooplankton fecal pellets: implications for substrate turnover by attached bacteria. Limnol. Oceanogr. 53, 1878–1886. https://doi.org/10.4319/lo.2008.53.5.1878.
Quast, C., Pruesse, E., Yilmaz, P., Gerken, J., Schweer, T., Yarza, P., Peplies, J., Glöckner, F.O., 2013. The SILVA ribosomal RNA gene database project: improved data processing and web-based tools. Nucleic Acids Res. 41, D590–D596. https://doi.org/10.1093/nar/gks1219.
Quigg, A., Passow, U., Chin, W.-C., et al., 2016. The role of microbial exopolymers in determining the fate of oil and chemical dispersants in the ocean. Limnol. Oceanogr. Lett. 3–26. https://doi.org/10.1002/lol2.10030.
Quigg, A., Sylvan, J.B., Gustafson, A.B., Fisher, T.R., Oliver, R.L., Tozzi, S., Ammerman, J.W., 2011. Going west: nutrient limitation of primary production in the Northern Gulf of Mexico and the importance of the Atchafalaya River. Aquat. Geochem. 17, 519–544. https://doi.org/10.1007/s10498-011-9134-3.
Ramachandran, S.D., Sweezey, M.J., Hodson, P.V., Boudreau, M., Courtenay, S.C., Lee, K., King, T., Dixon, J.A., 2006. Influence of salinity and fish species on PAH uptake from dispersed crude oil. Mar. Pollut. Bull. 52, 1182–1189. https://doi.org/10.1016/j.marpolbul.2006.02.009.
Reddy, C.M., Arey, J.S., Seewald, J.S., et al., 2012. Composition and fate of gas and oil released to the water column during the Deepwater Horizon oil spill. Proc. Natl. Acad. Sci. U. S. A. 109, 20229–20234. https://doi.org/10.1073/pnas.1101242108.
Rowe, G.T., Chapman, P., 2002. Continental shelf hypoxia: some nagging questions. Gulf Mex. Sci. 20, 153–160.
Sammarco, P.W., Kolian, S.R., Warby, R.A.F., Bouldin, J.L., Subra, W.A., Porter, S.A., 2013. Distribution and concentrations of petroleum hydrocarbons associated with the BP/Deepwater Horizon Oil Spill, Gulf of Mexico. Mar. Pollut. Bull. 73, 129–143. https://doi.org/10.1016/j.marpolbul.2013.05.029.
Schreiber, U., 1998. Chlorophyll fluorescence: new instruments for special applications. Photosynthesis: Mech. Effects 5, 4253–4258. https://doi.org/10.1007/978-94-011-3953-3_984.
Siron, R., Pelletier, É., Roy, S., 1996. Effects of dispersed and adsorbed crude oil on microalgal and bacterial communities of cold seawater. Ecotoxicology 5, 229–251. https://doi.org/10.1007/BF00118994.
Smith, P.K., Krohn, R.I., Hermanson, G.T., et al., 1985. Measurement of protein using bicinchoninic acid. Anal. Biochem. 150, 76–85. https://doi.org/10.1016/0003-2697(85)90442-7.
Sommer, U., 1994. Are marine diatoms favoured by high Si:N ratios? Mar. Ecol. Prog. Ser. 115, 309–315. https://doi.org/10.3354/meps115309.
Srivastava, A., Strasser, R.J., Govindjee, and, 1995. Differential effects of dimethylbenzoquinone and dichlorobenzoquinone on chlorophyll fluorescence transient in spinach thylakoids. J. Photochem. Photobiol. B Biol. 31, 163–169. https://doi.org/10.1016/1011-1344(95)07177-6.
Strom, S.L., Strom, M.W., 1996. Microplankton growth, grazing, and community structure in the northern Gulf of Mexico. Mar. Ecol. Prog. Ser. 130, 229–240. https://doi.org/10.2307/24855621.
Suggett, D.J., Moore, C.M., Hickman, A.E., Geider, R.J., 2009. Interpretation of fast repetition rate (FRR) fluorescence: signatures of phytoplankton community structure versus physiological state. Mar. Ecol. Prog. Ser. 376, 1–19. https://doi.org/10.3354/meps07830.
Tomas, C.R., 1997. In: Tomas, C.R. (Ed.), Identifying Marine Phytoplankton. Academic Press.
Von Der Heyden, S., Chao, E.E., Vickerman, K., Cavalier-Smith, T., 2004. Ribosomal RNA phylogeny of bodonid and diplonemid flagellates and the evolution of euglenozoa. J. Eukaryot. Microbiol. 51, 402–416. https://doi.org/10.1111/j.1550-7408.2004.tb00387.x.
Wade, T.L., Morales-McDevitt, M., Bera, G., others, 2017. A method for the production of large volumes of WAF and CEWAF for dosing mesocosms to understand marine oil snow formation. Heliyon 3, e00419. https://doi.org/10.1016/j.heliyon.2017.e00419.
Wade, T.L., Sweet, S.T., Sericano, J.L., et al., 2013. Analyses of Water samples from the deepwater horizon oil spill: documentation of the subsurface plume. Monitoring and Modeling the Deepwater Horizon Oil Spill: A Record Breaking Enterprise. American Geophysical Union, pp. 77–82.
White, H.K., Hsing, P.-Y., Cho, W., et al., 2012. Impact of the Deepwater Horizon oil spill on a deep-water coral community in the Gulf of Mexico. Proc. Natl. Acad. Sci. 109, 20303–20308. https://doi.org/10.1073/pnas.1118029109.
Wolfstein, K., Stal, L.J., 2002. Production of extracellular polymeric substances (EPS) by benthic diatoms: effect of irradiance and temperature. Marine Ecol. Prog. Series2 236, 13–22. https://doi.org/10.2307/24866271.
Wood, D.E., Salzberg, S.L., 2014. Kraken: ultrafast metagenomic sequence classification using exact alignments. Genome Biol. 15, R46. https://doi.org/10.1186/gb-2014-15-3-r46.
Xu, C., Zhang, S., Chuang, C., Miller, E.J., Schwehr, K.A., Santschi, P.H., 2011. Chemical composition and relative hydrophobicity of microbial exopolymeric substances (EPS) isolated by anion exchange chromatography and their actinide-binding affinities. Mar. Chem. 126, 27–36. https://doi.org/10.1016/j.marchem.2011.03.004.
Yamada, M., Takada, H., Toyoda, K., et al., 2003. Study on the fate of petroleum-derived polycyclic aromatic hydrocarbons (PAHs) and the effect of chemical dispersant using an enclosed ecosystem, mesocosm. Mar. Pollut. Bull. 105–113.
Yan, B., Passow, U., Chanton, J.P., et al., 2016. Sustained deposition of contaminants from the deepwater horizon spill. Proc. Natl. Acad. Sci. U. S. A. 113, E3332–40. https://doi.org/10.1073/pnas.1513156113.
Yemm, E.W., Willis, A.J., 1954. The estimation of carbohydrates in plant extracts by anthrone. Biochem. J. 57, 508–514. https://doi.org/10.1042/bj0570508.